Biochemical and Biophysical Research Communications 446 (2014) 410–416

Contents lists available at ScienceDirect

Biochemical and Biophysical Research Communications

journal homepage: www.elsevier.com/locate/ybbrc

GLP-1 promotes mitochondrial metabolism in vascular smooth muscle cells by enhancing endoplasmic reticulum–mitochondria coupling

Pablo E. Morales [1], Gloria Torres [1], Cristian Sotomayor-Flores, Daniel Peña-Oyarzún, Pablo Rivera-Mejías, Felipe Paredes, Mario Chiong *

Advanced Center for Chronic Diseases, Centro Estudios Moleculares de la Célula, Departamento Bioquímica y Biología Molecular, Facultad Ciencias Químicas y Farmacéuticas, Universidad de Chile, Santiago, Chile

ARTICLE INFO

Article history:
Received 27 February 2014
Available online 12 March 2014

Keywords:
GLP-1
VSMC
Mitochondrial metabolism
ER–mitochondria coupling
PKA
Mitofusin-2

ABSTRACT

Incretin GLP-1 has important metabolic effects on several tissues, mainly through the regulation of glucose uptake and usage. One mechanism for increasing cell metabolism is modulating endoplasmic reticulum (ER)–mitochondria communication, as it allows for a more efficient transfer of Ca^{2+} into the mitochondria, thereby increasing activity. Control of glucose metabolism is essential for proper vascular smooth muscle cell (VSMC) function. GLP-1 has been shown to produce varied metabolic actions, but whether it regulates glucose metabolism in VSMC remains unknown. In this report, we show that GLP-1 increases mitochondrial activity in the aortic cell line A7r5 by increasing ER–mitochondria coupling. GLP-1 increases intracellular glucose and diminishes glucose uptake without altering glycogen content. ATP, mitochondrial potential and oxygen consumption increase at 3 h of GLP-1 treatment, paralleled by increased Ca^{2+} transfer from the ER to the mitochondria. Furthermore, GLP-1 increases levels of Mitofusin-2 (Mfn2), an ER-mitochondria tethering protein, via a PKA-dependent mechanism. Accordingly, PKA inhibition and Mfn2 down-regulation prevented mitochondrial Ca^{2+} increases in GLP-1 treated cells. Inhibiting both Ca^{2+} release from the ER and Ca^{2+} entry into mitochondria as well as diminishing Mfn2 levels blunted the increase in mitochondrial activity in response to GLP-1. Altogether, these results strongly suggest that GLP-1 increases ER–mitochondria communication in VSMC, resulting in higher mitochondrial activity.

1. Introduction

The incretin GLP-1 (glucagon-like peptide-1) is a gut-derived peptide hormone with insulinotropic effects and extensive metabolic actions [1,2]. In skeletal muscle and liver, GLP-1 induces glycogenesis and glucose utilization [1,3,4], and in rat adipose tissue and cultured 3T3-L1 adipocytes, it is also able to induce lipogenesis [1,5]. In myocardial tissue, GLP-1 stimulates glucose uptake through an Akt-1-independent and p38-MAPK-dependent mechanism, by inducing translocation of GLUT-1 to the plasma membrane [6].

Moreover, mitochondria have a pivotal role in the regulation of cell metabolism, and its activity is finely regulated. In this regard, a rise in Ca^{2+} matrix levels induces an increase in mitochondrial activity through the activation of several Krebs cycle dehydrogenases, resulting in enhanced production of reducing power [7]. Ca^{2+} uptake into mitochondria requires high cytoplasmatic Ca^{2+} levels in the surrounding area, concentrations achieved in the proximity of Ca^{2+} release sites located in the endoplasmic reticulum (ER), such as the inositol trisphosphate receptor (InsP3R) [7,8]. We and others have shown that functional coupling between these organelles promotes efficient Ca^{2+} entry into mitochondria, resulting in a higher mitochondrial potential ($\Delta\psi_m$) and oxygen consumption [9]. The physical junction between the ER and mitochondria relies on Mitofusin-2 (Mfn2) and other proteins [10]. In fact, genetic ablation of Mfn2 results in disrupted ER–mitochondria communication and causes a decrease in both Ca^{2+} transfer and mitochondrial bioenergetics [7,9].

In spite of the large amount of data about GLP-1-dependent metabolic effects on hepatocytes, adipocytes and skeletal muscle cells, to date there is no information available on direct effects of GLP-1 on glucose utilization, glycogen synthesis or mitochondrial regulation in vascular smooth muscle cells (VSMC). VSMC are the main component of the artery's medial layer. These cells contract to regulate blood vessel tone and consequently blood flow and

* Corresponding author. Address: ACCDiS, CEMC, Universidad de Chile, Sergio Livingstone P 1007, Santiago 8380492, Chile.
E-mail address: mchiong@uchile.cl (M. Chiong).
[1] Both authors contributed equally to this work.

http://dx.doi.org/10.1016/j.bbrc.2014.03.004
0006-291X/

pressure. Because glucose metabolism is a key player in vascular reactivity [11], the metabolic effects of GLP-1 on VSMC could be relevant in the control of vascular function.

In this report, we show that GLP-1 treatment augments Mfn2 levels through a PKA-dependent mechanism, resulting in increased ER–mitochondria communication and enhanced mitochondrial activity in VSMC. Our results reveal a new mechanism by which GLP-1 controls cell metabolism.

2. Materials and methods

2.1. Cell culture

The A7r5 cell line, originally derived from embryonic rat aorta, was purchased from the American Type Culture Collection (ATCC). The cell line was cultured in DMEM supplemented with 10% fetal bovine serum (FBS) and 2 mM pyruvate. Prior to stimulation, 80–90% confluent VSMCs were serum-starved overnight by incubating in DMEM without FBS. Cells were stimulated with GLP-1 (7–36) amide (American Peptide Company, Sunnyvale, CA) 100 nM.

2.2. Glucose metabolism

Cells were rinsed twice with HEPES-buffer saline (in mM: 140 NaCl; 20 HEPES-Na; 5 KCl; 2.5 $MgSO_4$, 1 $CaCl_2$, pH 7.4), and then glucose uptake was determined using [^{3}H]-2-deoxyglucose ([^{3}H]-2-DOG, Perkin Elmer) as described [12]. Glucose and glycogen were measured with a colorimetric-based kit (Glycogen Assay Kit, BioVision) following manufacturer instructions.

2.3. Mitochondria and ER imaging

After stimulation with GLP-1, cells were incubated with Mitotracker Orange (400 nM for 30 min), washed with PBS, fixed with paraformaldehyde (4% [w/v] in PBS for 20 min), permeabilized with Triton X-100 (0.1% [v/v] in PBS for 10 min) and blocked with bovine serum albumin (BSA, 1% [w/v] in PBS for 1 h). For ER detection, cells were incubated with anti-KDEL antibody (1:500 in PBS-BSA overnight) and revealed with anti IgG-Alexa 488 (1:500 in PBS-BSA for 2 h). Confocal images were captured with a Zeiss LSM-5, Pascal 5 Axiovert 200, equipped with a Plan-Apochromat 63 × /1.4 Oil DIC objective and with LSM 5 3.2 software for image capture/analysis. Colocalization between organelles was quantified using the Manders' algorithm [13].

2.4. RNA isolation and real-time PCR

Total RNA (1 μg), extracted from culture cells by using Trizol, was used to synthesize the first-strand cDNA with the MuLV Reverse Transcriptase and random primers. The following primers were used: *Glp-1r* forward primer (TGT ACC TGA GCA TAG GCT GG), *Glp-1r* reverse primer (GCT CCC AGC TCT TCC GAA AC), *Mfn2* forward primer (CAT GTC CAT GAT GCC CAA CC), *Mfn2* reverse primer (TTC TTG ACG GTG ACG ATG GAG), *Gapdh* forward primer (CCA TGG AGA AGG CTG GGG) and *Gapdh* reverse primer (CAA AGT TGT CAT GGA TGA CC). The conditions used for all PCRs were 95 °C for 3 s, 52 °C for 15 s and 72 °C for 25 s. qPCR were performed by using the Brilliant II SYBR Green QPCR Master Mix (Agilent Technologies).

2.5. Mitochondrial activity

For measurement of mitochondrial membrane potential ($\Delta\psi_m$), A7r5 cells were loaded with 10 μM JC-1 for 15 min. Fluorescence was analyzed immediately by flow cytometry in a Becton Dickinson FACSort cytometer (λ_{exc} = 488 nm, λ_{em} = 530 and 590 nm). ROS was measured using 2′-7′-dihydrochlorofluorescein (5 μM) by flow cytometry (fluorescence λ_{exc} = 492–495 nm and λ_{em} = 517–527 nm). ATP content was determined using a luciferin/luciferase based assay (Cell-Titer Glo Kit, Promega) following manufacturer instructions. Oxygen consumption was determined in trypsinized cells using a Clark electrode 5331 (Yellow Springs Instruments). Maximum rate oxygen consumption in all conditions was determined using carbonyl cyanide m-chlorophenyl-hydrazone (CCCP) 200 nM.

2.6. Measurement of mitochondrial Ca^{2+} uptake

Mitochondrial Ca^{2+} images were obtained from A7r5 cells preloaded with RhodFF-AM (5,4 μM) using an inverted confocal microscope (Carl Zeiss Axiovert 135M-LSM Microsystems). The fluorescent images were collected every 0.985 s. Mitochondrial Ca^{2+} was expressed as a percentage of fluorescence intensity relative to baseline fluorescence.

2.7. Western blot analysis

Equal amounts of protein from cells were separated by SDS–PAGE (10% polyacrylamide gels) and electrotransferred to nitrocellulose. Membranes were blocked with 5% milk in Tris-buffered saline, pH 7.6, containing 0.1% (v/v) Tween 20 (TBST). Membranes were incubated with primary antibodies at 4 °C (Mfn2 1:1000; total CREB 1:000, pCREB Ser^{133} 1:1000, total Akt 1:1000, pAkt Ser^{473} 1:1000, pPDH Ser^{293} 1:1000, total PDH 1:1000, GLP-1R 1:2000, α-SMA 1:50,000) and re-blotted with horseradish peroxidase-linked secondary antibody (1:5000 in 1% [w/v] milk in TBST). The bands were detected using ECL with exposure to Kodak film and quantified by scanning densitometry. Protein content was normalized by β-tubulin.

2.8. Statistical analysis

Data are shown as mean ± SEM of the number of independent experiments indicated (n). Data were analyzed by Student's t-test or one-way ANOVA (3 or more groups), and comparisons between groups were performed using a protected Dunnett's test. When inhibitors or siRNA were used, two-way ANOVA followed with Bonferroni's post-test was applied. Statistical significance was defined as $p < 0.05$.

3. Results

3.1. GLP-1 regulates glucose metabolism in VSMC

Unlike insulin stimulation, GLP-1 did not increase glucose uptake in a period of time ranging from 0 to 60 min (Fig. 1A, Supplemental Fig. 1A). However, when assessed the effect of long times of GLP-1 exposure, we observed a significant decrease in glucose uptake at 3 h of treatment (Fig. 1B). We also observed that GLP-1 increased glucose content at 3 h (Fig. 1C), while no significant alteration in glycogen levels were detected (Fig. 1D). Similar results were obtained in primary cultured rat mesenteric artery smooth muscle cells (maSMC) (Supplemental Fig. 1B). Inactivating PDH-Ser^{293}-phosphorylation was diminished at 3 h of GLP-1 treatment (Fig. 1E), suggesting a redirectionation of glucose metabolism to the mitochondria. Taken together, these results show that in VSMC, GLP-1 decreases glucose uptake and promotes glucose accumulation, probably by redirecting cytosolic glucose metabolism to the mitochondria.

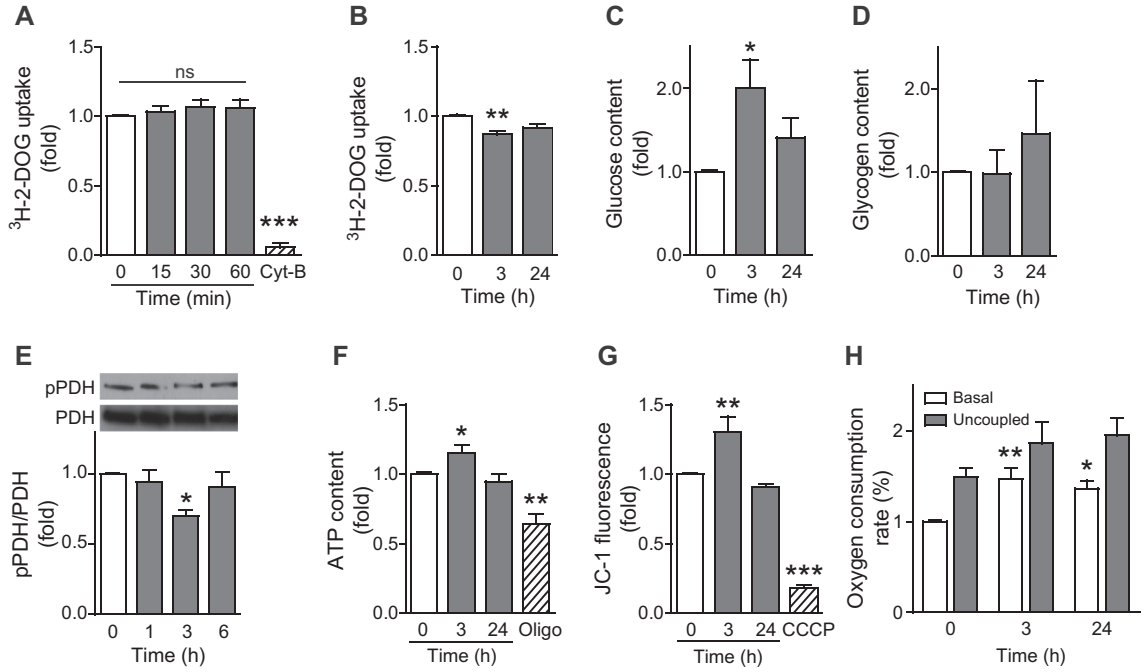

Fig. 1. GLP-1 regulates glucose metabolism and promotes mitochondrial activity in VSMC. (A) A7r5 cells were stimulated with GLP-1 for 0–60 min. (B) A7r5 cells were stimulated for 0–24 h with GLP-1. Glucose uptake was determined using [^{3}H]-2-deoxyglucose ([^{3}H]-2-DOG). Cytochalasin-B (10 μM) was used as a control to determine non-specific glucose transport. Glucose (C) and glycogen (D) contents were measured as indicated in Section 2. (E) Cells were stimulated for 0, 3 and 24 h with GLP-1 and then phosphorylated (pPDH) and total PDH were determined by Western blot. (F) ATP content was measured by a luciferin/luciferase-based kit. Oligomycin (Oligo, 2 μM) was added for 1 h as an experimental control. (G) Mitochondrial potential ($\Delta\psi_m$) was determined using JC-1 probe (10 μM) and detected using a FACS system. Uncoupler CCCP (200 nM) was used as a control. (H) A7r5 cells were stimulated for 0, 3 and 24 h with GLP-1. Oxygen consumption rate was measured for 5 min (basal oxygen consumption – white bars), and then CCCP (200 nM) was added to the polarographic chamber for another 5 min (uncoupled oxygen consumption – gray bars). Data are the average ± SEM of 4–5 independent experiments and are presented as fold vs. control $^*p < 0.05$ vs. 0 h or control; $^{**}p < 0.01$vs. 0 h; and $^{***}p < 0.001$ vs. 0 h.

3.2. GLP-1 promotes mitochondrial activity in VSMC

GLP-1 increased intracellular levels of ATP, $\Delta\psi_m$ and oxygen consumption at 3 h of treatment (Fig. 1F–H). Raise in oxygen consumption was not due to an increased mitochondrial oxidative capacity, because CCCP-stimulated maximal oxygen consumption was not significantly modified with GLP-1 treatment (Fig. 1H). We did not observe changes in ROS levels after GLP-1 treatment (Supplemental Fig. 1C), suggesting an efficient coupling among the components of the electron transport chain. In maSMC, $\Delta\psi_m$ was also enhanced by GLP-1 treatment (Supplemental Fig. 1D). Collectively, these data suggest that GLP-1 enhances mitochondrial activity in VSMC.

3.3. GLP-1 increases functional coupling between mitochondria and the endoplasmic reticulum

To test whether the increased mitochondrial activity was correlated with enhanced ER–mitochondria communication, A7r5 cells were incubated with GLP-1 and stained with Mitotracker Orange and anti-KDEL antibody, to visualize mitochondrial and ER networks, respectively (Fig. 2A). At 3 h of GLP-1 treatment, an increased colocalization of these signals was observed, as determined by an increase in the mitochondria-over-ER Manders' coefficient (Fig. 2B). These results suggest that GLP-1 induces an increase in ER–mitochondria contacts.

To evaluate functionality of mitochondria–ER contacts, we measured mitochondrial Ca^{2+} levels in response to histamine stimulation, which induces Ca^{2+} release from the ER by InsP3R [8]. In both control and cells stimulated with GLP-1 for 3 h, histamine increased mitochondrial Ca^{2+} levels (Fig. 2C). However, this increase was higher in cells pre-treated with GLP-1. The area under curve, as an index of the Ca^{2+} influx to the mitochondria, was significantly increased (Fig. 2D). Accordingly, mitochondrial Ca^{+2} intake velocity also increased nearly 2-fold (Fig. 2E). We also measured the level of mitochondrial calcium uniporter (MCU), as it is responsible for Ca^{2+} intake into mitochondria [14], and observed no significant changes (Fig. 2F). Histamine also induced Ca^{2+} release from the ER in maSMC and transfer to mitochondria was increased in GLP-1-treated cells (Supplemental Fig. 2A–C). Collectively, increased colocalization of ER and mitochondria, along with the higher area under curve and Ca^{2+} intake velocity, suggest a closer contact between ER and mitochondria. Therefore, we conclude that GLP-1 promotes functional coupling between these organelles, allowing for a more efficient Ca^{2+} transfer from ER to mitochondria in VSMC.

3.4. Activation of the GLP-1R/PKA/Mfn2 pathway by GLP-1

GLP-1 receptor (GLP-1R) is not ubiquitously expressed, and although it has been found in rat mesenteric artery [15], no information is available regarding its expression in A7r5 cell line. By qPCR, we were able to detect *Glp-1r* mRNA on these cells and observed no changes in response to GLP-1 (Fig. 3A, upper panel). In parallel, GLP-1R protein levels were visualized by Western blotting (Fig. 3A, medium panel) and showed no significant variations upon GLP-1 treatment (Fig. 3A, lower panel).

GLP-1, unlike insulin, did not induce Akt phosphorylation (Supplemental Fig. 3A), suggesting that GLP-1 does not activate the PI3K/Akt pathway in this cell line. Next, we evaluated PKA activation by measuring Ser^{133}-CREB phosphorylation (pCREB), a known downstream effector of PKA [16]. GLP-1 induced an increase in pCREB levels with a peak at 15 min post stimulus (Fig. 3B). CREB phosphorylation was due to PKA activation, as pre-treatment with the PKA specific inhibitor, H-89, completely abolished GLP-1 response (Supplemental Fig. 3B).

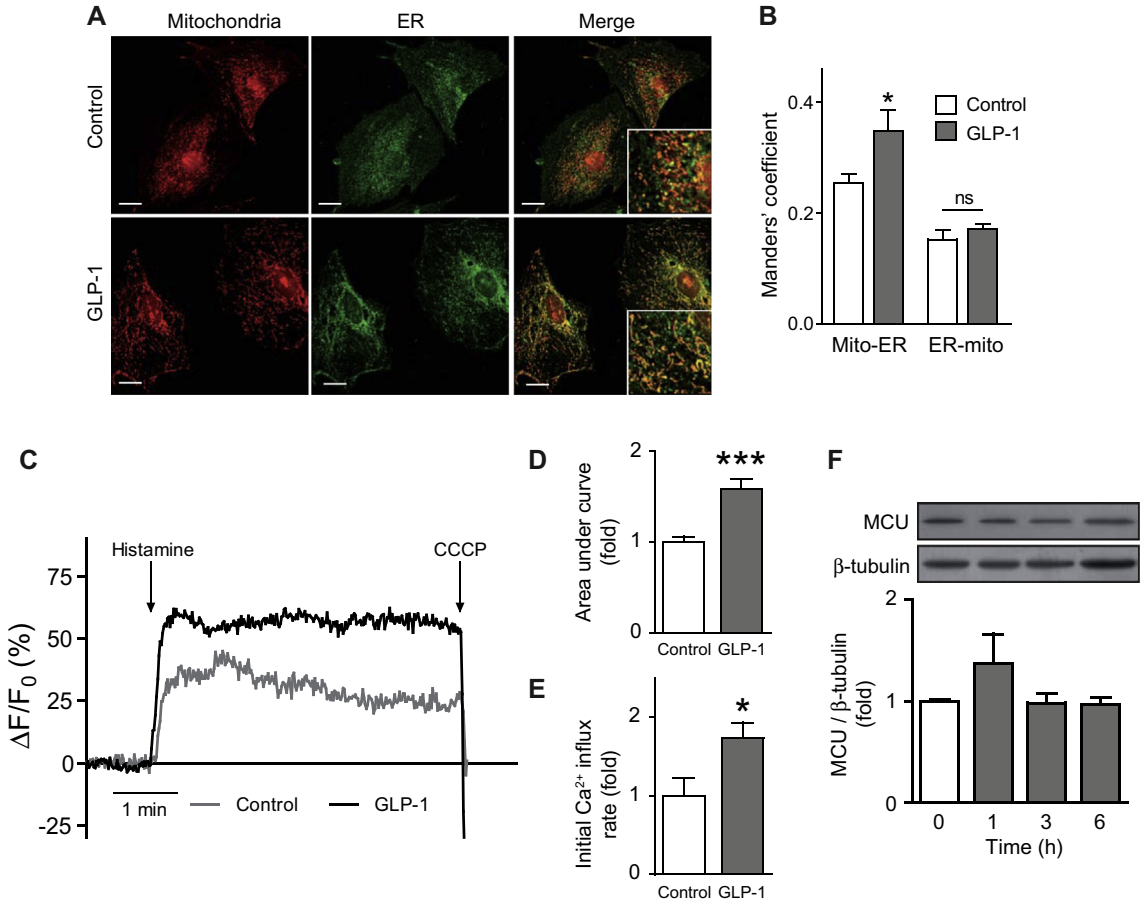

Fig. 2. GLP-1 enhances ER–mitochondria coupling. A7r5 cells were treated or not (control) with GLP-1 for 3 h and visualized by confocal microscopy. (A) Representative images by confocal microscopy of A7r5 cells. Mitochondria and ER were labeled with Mitotracker orange (400 nM) and KDEL antibody 1:500 (green), respectively. Bar represents 10 μm. (B) Colocalization was assessed by Manders' coefficients of mitochondria over reticulum (Mito-ER) and reticulum over mitochondria (ER-Mito). (C) Mitochondrial Ca^{2+} levels after histamine (100 μM) stimulation was evaluated by change in fluorescence of RhodFF probe (5.4 μM) by confocal microscopy with respect to baseline ($\Delta F/F_0$). Fluorescent images were collected every 0.985 s and analyzed frame-by-frame with Image J software. Cells with GLP-1 treatment (black) were compared with control (gray). Area under the curve (D) and initial Ca^{2+} influx velocity (E) were determined from (C). (F) A7r5 cells were stimulated 0–6 h with GLP-1 and then MCU total levels were determined by Western blot. Data are the average ± SEM of 4–5 independent experiments. $^{*}p < 0.05$ and $^{***}p < 0.001$ vs. control.

GLP-1 increased Mfn2 levels near 2-fold at 3 h of stimulation (Fig. 3C). Additionally, H-89 pre-treatment inhibited this increase, suggesting PKA-dependence in the regulation of Mfn2 levels by GLP-1 (Supplemental Fig. 3C). We measured Mfn2 mRNA levels in response to GLP-1 and observed a significant increase as soon as 1 h of treatment, suggesting a genomic-mediated response (Supplemental Fig. 3D). Therefore, our results show that GLP-1 activates a GLP-1R/PKA dependent pathway and regulates Mfn2 protein levels. These results prompted us to evaluate PKA and Mfn2 as mediators of the enhanced coupling of ER and mitochondria in response to GLP-1.

3.5. Increased ER-Ca^{2+} transfer to mitochondria by GLP-1 depends on PKA activity and Mfn2 levels

To evaluate the role of PKA and Mfn2 in the GLP-1 dependent enhanced coupling between ER and mitochondria, we measured mitochondrial Ca^{2+} levels in response to histamine in H-89 and siRNA Mfn2 pre-treated cells. GLP-1 increased Ca^{2+} entry into mitochondria in response to histamine, but this effect was blunted by PKA inhibition (Fig. 3D and E) and with two different siRNAs against Mfn2 (Fig. 3F, G and Supplemental Fig. 3F, G). These data show that increased coupling between the ER and mitochondria stimulated by GLP-1 depends on PKA activity and Mfn2 levels.

3.6. Functional ER–mitochondria coupling regulates GLP-1-induced mitochondrial activity

Specific inhibition of InsP3R with xestospongin-B completely blunted the increase in $\Delta\psi_m$ and oxygen consumption in GLP-1-treated cells (Fig. 4A). The same results were observed when ruthenium red, an MCU blocker, was used (Fig. 4B). In agreement with our previous results, PKA inhibition with H-89 abolished the increase in $\Delta\psi_m$ and oxygen consumption in response to GLP-1 (Fig. 4C). To demonstrate GLP-1R involvement, we pre-treated cells with Ex9 and observed no response to GLP-1 when $\Delta\psi_m$ was measured (Fig. 4D). Finally, we observed that siMfn2-treated cells were unable to respond to GLP-1 (Fig. 4E), indicating that increased Mfn2 levels are necessary for GLP-1 action. Collectively, these data show that Ca^{2+} transfer from the ER to mitochondria is fundamental for increased mitochondrial activity in GLP-1 stimulated cells, and that this process relies on GLP-1R activation, PKA activity and increased Mfn2 levels.

4. Discussion

In VSMC, glucose metabolism is emerging as a fundamental biological process, important for controlling not only cell function but also cell phenotype [11]. Our findings are the first to show that

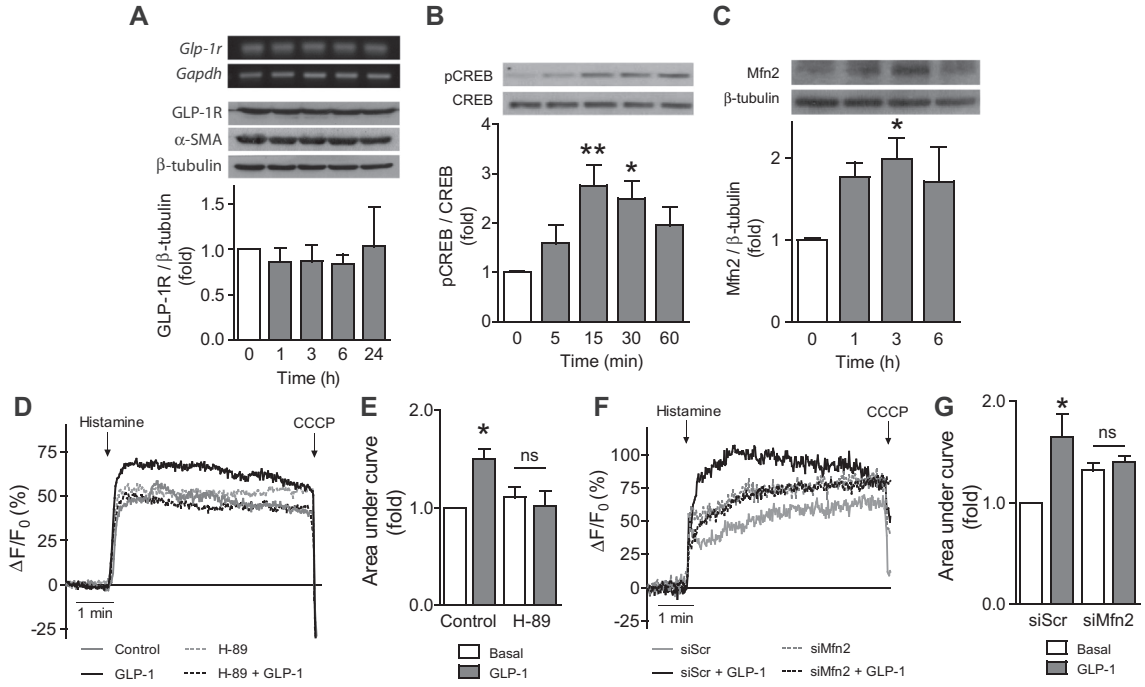

Fig. 3. GLP-1 induces mitochondria–ER Ca^{2+} transfer through a PKA/Mfn2-dependent mechanism. (A) A7r5 cells were treated with GLP-1 for the indicated times and then qPCR or Western blot experiments were performed. Upper panel: agarose gel for *Glp-1r* cDNA visualization. *Gapdh* was used as a loading control. Medium and lower panel: Western blot for GLP-1R. α-SMA was used as a smooth muscle marker and β-tubulin was used as a loading control. (B) PKA activity was evaluated by CREB phosphorylation using Western blot. (C) Mitofusin 2 (Mfn2) total levels were measured by Western blot. Data were normalized using β-tubulin. (D) A7r5 cells were treated with GLP-1 (solid black), H-89 (10 μM) (dashed gray) or GLP-1 + H-89 (dashed black), loaded with RhodFF-AM (5.4 μM) for 30 min and then analyzed using confocal microscopy. Release of Ca^{2+} from the ER was performed using histamine (100 μM). Non-treated cells were used as a control (solid gray). (F) A7r5 cells were treated with scramble siRNA (siScr) (solid gray), scramble siRNA (siScr) + GLP-1 (solid black), siRNA Mfn2 (siMfn2) (dashed gray) or siMfn2 + GLP-1 (dashed black) and treated as indicated in (D). CCCP was used as a control. (E) and (G) Area under the curves of graphs (D) and (F), respectively. Data are the average ± SEM of 4–5 independent experiments. $^{*}p < 0.05$; and $^{**}p < 0.01$ vs. 0 h or baseline.

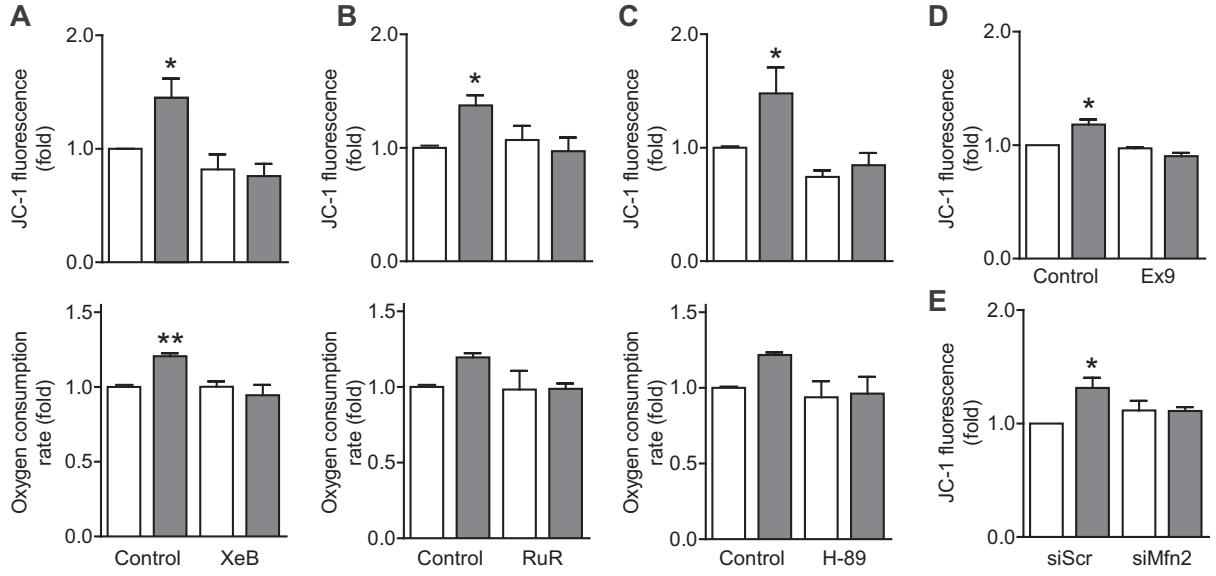

Fig. 4. GLP-1-dependent enhanced ER–mitochondria coupling increases mitochondrial activity. A7r5 cells were pre-treated for 30 min with (A) xestospongin b (XeB, InsP3R antagonist), (B) ruthenium red (RuR, MCU blocker), (C) H-89 (PKA inhibitor) or (D) Exendin (9–39) (Ex9, GLP-1R antagonist) and then stimulated with (gray bars) or without (white bars) GLP-1 for 3 h. (E) A7r5 cells were treated with scramble siRNA (siScr) or Mfn2 siRNA (siMfn2) for 24 h and then incubated with (gray bars) or without (white bars) GLP-1 for 3 h. Mitochondrial potential (JC-1 fluorescence) and oxygen consumption (Clark electrode) were determined. Data are the average ± SEM of 4 independent experiments. $^{*}p < 0.05$ vs. without GLP-1.

GLP-1 controls glucose metabolism by regulating ER–mitochondria interaction in VSMC. GLP-1 activates GLP-1R, promotes PKA activation and increases Mfn2, leading to an enhanced Ca^{2+} transfer from the ER to mitochondria. Increased Ca^{2+} boosts mitochondrial metabolism, resulting in enhanced $\Delta\psi_m$, ATP levels and O_2 consumption (Supplemental Fig. 4).

Extrapancreatic insulin-like effects of GLP-1 have been described in liver, skeletal muscle, cultured cardiomyocytes and

adipose tissue, where it promotes glycogen synthesis and glucose utilization [1–3]. Unexpectedly, here we showed that GLP-1 did not increase, but rather decreased, glucose uptake in VSMC. Moreover, no alteration in glycogen content was observed in VSMC upon GLP-1 treatment.

VSMC exhibit unusually high rates of glucose metabolization and lactate production under normal, well-oxygenated conditions [17]. Besides diminished glucose uptake, GLP-1 treatment increased intracellular glucose level without modification of glycogen content, suggesting that glucose utilization is diminished. This could be explained if glucose was not mainly metabolized through anaerobic glycolysis, but allowed to continue to further mitochondrial oxidation. Accordingly, we observed that the inactivating phosphorylation of PDH, the rate-limiting enzyme responsible for connecting cytosolic to mitochondrial oxidation of glucose, was diminished. Furthermore, an increase in mitochondrial activity could maintain cell bioenergetics (i.e., intracellular ATP content) with a reduction in anaerobic glucose utilization. This seems to be the case, as our results showed that GLP-1 treatment induced an increase in intracellular ATP, paralleled with increased $\Delta\psi_m$ and O_2 consumption, all parameters consistent with mitochondrial activation. Therefore, our results suggest that GLP-1 induced a metabolic shift in VSMC as it redirects glucose metabolization to a more efficient process, leading to glucose accumulation and increased mitochondrial metabolism. The signaling pathway involved in the increased mitochondrial metabolism seems to be associated with the classical cascade activated by GLP-1, i.e., GLP-1R/PKA. We observed that GLP-1R is efficiently expressed in A7r5 cells and that upon GLP-1 stimulation, PKA activation was observed.

One possible mechanism for promoting mitochondrial activity is raising mitochondrial Ca^{2+} levels [18,19]. Increased mitochondrial Ca^{2+} concentration enhances oxidative phosphorylation, mediated by the activation of four mitochondrial dehydrogenases: FAD-glycerol 3-phosphate dehydrogenase, pyruvate dehydrogenase, NAD-isocitrate dehydrogenase and oxoglutarate dehydrogenase [18]. In order to trigger Ca^{2+} release from InsP3R and measure Ca^{2+} transfer from ER to the mitochondria, we used histamine [8]. Using this procedure, we showed that GLP-1 induced a functional coupling between ER and mitochondria in VSMC, as it promoted a faster and higher increase of mitochondrial Ca^{2+} entry in histamine-treated cells. This enhanced coupling was associated with an increase in mitochondrial metabolism because inhibition of Ca^{2+} release from ER using the InsP3R blocker xestospongin B or the blockade of Ca^{2+} entry to the mitochondria using RuRed abolished GLP-1-dependent increase of O_2 consumption and $\Delta\psi_m$. Presumably, the involvement of InsP3R in the GLP-1 response is a consequence of the basal leakage of Ca^{2+} from the ER, as it has been shown that this Ca^{2+} release is responsible for maintaining a constitutive mitochondrial metabolism [19]. Pulmonary smooth muscle cells also preferentially use glucose to obtain energy, and promoting mitochondrial glucose oxidation prevents proliferation and remodeling [20,21]. In these cells, glucose oxidation can be reduced by increasing the distance between mitochondria and ER [21]. Therefore, it seems that functional communication between mitochondria and the ER is an efficient mechanism for promoting mitochondrial metabolism and regulating VSMC phenotype.

Mitochondria connection to the ER is mediated by Mfn2 [7,10]. Mfn2 tethers mitochondria to the ER, and Mfn2 overexpression increases functional coupling between these two organelles [7,10]. Here we show that GLP-1 increased Mfn2 mRNA and protein levels. Furthermore, we observed that this response requires PKA activation. Guo et al. observed that forskolin increases Mfn2 expression en VSMC [22]. Our results totally agree with this report, and confirm the involvement of PKA in regulation of Mfn2 levels. Our results show that silencing Mfn2 decreased Ca^{2+} influx to the mitochondria, with a consequent decrease in $\Delta\psi_m$. These results suggest that in VSMC, Mfn2 is also important in glucose metabolism.

In conclusion, our results suggest that the vascular action of GLP-1 involves a metabolic shift in VSMC, enhancing mitochondrial activity, triggered by a GLP-1R/PKA/Mfn2-dependent increased mitochondria–ER communication.

Acknowledgments

This research was funded in part by Comision Nacional de Ciencia y Tecnologia (CONICYT), Chile (FONDECYT 1110180 to M.C.; ANILLO ACT1111 to M.C.; FONDAP 15130011 to M.C.). P.M. holds a CONICYT Master fellowship. G.T. and F.P. hold a CONICYT Ph.D. fellowship.

Appendix A. Supplementary data

Supplementary data associated with this article can be found, in the online version, at http://dx.doi.org/10.1016/j.bbrc.2014.03.004.

References

[1] J.E. Campbell, D.J. Drucker, Pharmacology, physiology, and mechanisms of incretin hormone action, Cell Metab. 17 (2013) 819–837.
[2] L.K. Phillips, J.B. Prins, Update on incretin hormones, Ann. NY. Acad. Sci. 1243 (2011) E55–E74.
[3] N. Gonzalez, A. Acitores, V. Sancho, I. Valverde, M.L. Villanueva-Penacarrillo, Effect of GLP-1 on glucose transport and its cell signalling in human myocytes, Regul. Pept. 126 (2005) 203–211.
[4] M. Morales, M.I. Lopez-Delgado, A. Alcantara, M.A. Luque, F. Clemente, L. Marquez, J. Puente, C. Vinambres, W.J. Malaisse, M.L. Villanueva-Penacarrillo, I. Valverde, Preserved GLP-I effects on glycogen synthase a activity and glucose metabolism in isolated hepatocytes and skeletal muscle from diabetic rats, Diabetes 46 (1997) 1264–1269.
[5] Y. Wang, H.K. Kole, C. Montrose-Rafizadeh, R. Perfetti, M. Bernier, J.M. Egan, Regulation of glucose transporters and hexose uptake in 3T3-L1 adipocytes: glucagon-like peptide-1 and insulin interactions, J. Mol. Endocrinol. 19 (1997) 241–248.
[6] S. Bhashyam, A.V. Fields, B. Patterson, J.M. Testani, L. Chen, Y.T. Shen, R.P. Shannon, Glucagon-like peptide-1 increases myocardial glucose uptake via p38alpha MAP kinase-mediated, nitric oxide-dependent mechanisms in conscious dogs with dilated cardiomyopathy, Circ. Heart Fail. 3 (2010) 512–521.
[7] R. Bravo-Sagua, A.E. Rodriguez, J. Kuzmicic, T. Gutierrez, C. Lopez-Crisosto, C. Quiroga, J. Diaz-Elizondo, M. Chiong, T.G. Gillette, B.A. Rothermel, S. Lavandero, Cell death and survival through the endoplasmic reticulum–mitochondrial axis, Curr. Mol. Med. 13 (2013) 317–329.
[8] G. Csordas, A.P. Thomas, G. Hajnoczky, Quasi-synaptic calcium signal transmission between endoplasmic reticulum and mitochondria, EMBO J. 18 (1999) 96–108.
[9] R. Bravo, J.M. Vicencio, V. Parra, R. Troncoso, J.P. Munoz, M. Bui, C. Quiroga, A.E. Rodriguez, H.E. Verdejo, J. Ferreira, M. Iglewski, M. Chiong, T. Simmen, A. Zorzano, J.A. Hill, B.A. Rothermel, G. Szabadkai, S. Lavandero, Increased ER–mitochondrial coupling promotes mitochondrial respiration and bioenergetics during early phases of ER stress, J. Cell Sci. 124 (2011) 2143–2152.
[10] O.M. de Brito, L. Scorrano, Mitofusin 2 tethers endoplasmic reticulum to mitochondria, Nature 456 (2008) 605–610.
[11] M. Chiong, P. Morales, G. Torres, T. Gutierrez, L. Garcia, M. Ibacache, L. Michea, Influence of glucose metabolism on vascular smooth muscle cell proliferation, Vasa 42 (2013) 8–16.
[12] A. Klip, T. Ramlal, P.J. Bilan, G.D. Cartee, E.A. Gulve, J.O. Holloszy, Recruitment of GLUT-4 glucose transporters by insulin in diabetic rat skeletal muscle, Biochem. Biophys. Res. Commun. 172 (1990) 728–736.
[13] E.M.M. Manders, E.J. Verbeek, J.A. Aten, Measurement of co-localization of objects in dual-colour confocal images, J. Microsc. 169 (1993) 375–382.
[14] J.M. Baughman, F. Perocchi, H.S. Girgis, M. Plovanich, C.A. Belcher-Timme, Y. Sancak, X.R. Bao, L. Strittmatter, O. Goldberger, R.L. Bogorad, V. Koteliansky, V.K. Mootha, Integrative genomics identifies MCU as an essential component of the mitochondrial calcium uniporter, Nature 476 (2011) 341–345.
[15] K. Ban, M.H. Noyan-Ashraf, J. Hoefer, S.S. Bolz, D.J. Drucker, M. Husain, Cardioprotective and vasodilatory actions of glucagon-like peptide 1 receptor are mediated through both glucagon-like peptide 1 receptor-dependent and -independent pathways, Circulation 117 (2008) 2340–2350.
[16] A.J. Shaywitz, M.E. Greenberg, CREB: a stimulus-induced transcription factor activated by a diverse array of extracellular signals, Annu. Rev. Biochem. 68 (1999) 821–861.

[17] T.M. Butler, M.J. Siegman, High-energy phosphate metabolism in vascular smooth muscle, Annu. Rev. Physiol. 47 (1985) 629–643.
[18] R.M. Denton, Regulation of mitochondrial dehydrogenases by calcium ions, Biochim. Biophys. Acta 1787 (2009) 1309–1316.
[19] C. Cardenas, R.A. Miller, I. Smith, T. Bui, J. Molgo, M. Muller, H. Vais, K.H. Cheung, J. Yang, I. Parker, C.B. Thompson, M.J. Birnbaum, K.R. Hallows, J.K. Foskett, Essential regulation of cell bioenergetics by constitutive InsP3 receptor Ca^{2+} transfer to mitochondria, Cell 142 (2010) 270–283.
[20] G. Sutendra, S. Bonnet, G. Rochefort, A. Haromy, K.D. Folmes, G.D. Lopaschuk, J.R. Dyck, E.D. Michelakis, Fatty acid oxidation and malonyl-CoA decarboxylase in the vascular remodeling of pulmonary hypertension, Sci. Transl. Med. 2 (2010) 44ra58.
[21] G. Sutendra, P. Dromparis, P. Wright, S. Bonnet, A. Haromy, Z. Hao, M.S. McMurtry, M. Michalak, J.E. Vance, W.C. Sessa, E.D. Michelakis, The role of Nogo and the mitochondria–endoplasmic reticulum unit in pulmonary hypertension, Sci. Transl. Med. 3 (2011) 88.
[22] X. Guo, K.H. Chen, Y. Guo, H. Liao, J. Tang, R.P. Xiao, Mitofusin 2 triggers vascular smooth muscle cell apoptosis via mitochondrial death pathway, Circ. Res. 101 (2007) 1113–1122.